

Jacobs Journal of Molecular and Translational Medicine

Original Article

Functional Ultrasound Imaging of Cerebral Capillaries in Rodents and Humans

Alan URBAN^{1,*,#}, Clément BRUNNER^{1,2,#}, Clara DUSSAUX¹, Francine CHASSOUX³, Bertrand DEVAUX³ and Gabriel MONT-ALDO^{1,3}

¹Optogenetics and Brain Imaging, Stroke Research Team, UMR5 894 INSERM Centre de Psychiatrie et Neurosciences, Faculté de Médecine, Université Paris Descartes, Sorbonne Paris Cité, Paris, France.

²Sanofi Research and Development, Lead Generation to Candidate Realization, Chilly-Mazarin, France.

³Department of Neurosurgery, Sainte-Anne Hospital Center, Université Paris Descartes Sorbonne Paris Cité, Paris, France.

[#]These authors contributed equally to this work.

*Corresponding author: Alan Urban, Optogenetics and Brain Imaging Group, Université Paris Descartes Sorbonne Paris Cité, Centre de Psychiatrie et Neurosciences, INSERM U894, Centre Hospitalier Sainte-Anne, Paris, France. Tel: +33140789277;

Email: alan.urban@alan-urban.fr

Received: 08-25-2015

Accepted: 10-27-2015

Published: 11-12-2015

Copyright: © 2015 A. URBAN

Abstract

Monitoring capillary blood flow is of great clinical value since microcirculation is crucial for proper delivery of oxygen and nutrients to the biological tissue, particularly in the brain. Functional ultrasound imaging is a novel method to measure hemodynamics in small vessels at a high resolution providing new insight into brain activity. Nevertheless, a drawback of this modality is the need for clutter filtering to suppress signals originating from slowly moving tissue that may hinder not only the detection of low blood flow velocity in micro vessels but also significantly underestimate the power spectrum of the Doppler signal. Here, we demonstrate how a spatiotemporal filtering approach based on the Singular Value Decomposition (SVD) can efficiently remove the clutter signal while preserving the blood flow signal even at low frequency. This strategy was applied to image brain capillaries in rodents and to visualize the cortical microvasculature in the human brain during neurosurgery.

Keywords: Cerebral Blood Flow; Cerebral Blood Volume (CBV); functional ultrasound; Singular Value Decomposition (SVD)

Introduction

Doppler Ultrasound imaging is a widely used technique for making non-invasive velocity measurements of blood flow. In this technique, the signal scattered from blood is added to signals scattered from stationary or slowly moving tissue that is typically 40 to 60 dB stronger than the signal from blood cells [1]. The echo signal of moving blood cells has a larger Doppler shift than the echoes reflected from slowly moving tissue and therefore it is possible to separate both signals using various static high-pass filters [2-5]. Neverthe-

less, the clutter from tissue often change through space and time due to change in physiology that can be overcome using adaptive filters based on principal component analysis [6-8].

In addition, it should be noted that none of these filtering strategies could effectively suppress the clutter without affecting the flow signal of interest. For example, a direct consequence of the clutter filter is the inability to detect all particles with a Doppler shift lower than the filter cut-off frequency. Then, all micro vessels with slow blood velocities below few mm/s including capillaries, arterioles and venules

are basically not detected using standard ultrasound scanners.

A dense vascular network with blood vessels varying in diameter and length irrigates the brain. For example, cortical vessels are basically divided in different categories: large pial vessels located on the surface (diameter > 100 μm ; blood velocity up to 34 mm/s) [9], penetrating arterioles and venules oriented perpendicularly to the surface (diameter 15-50 μm ; blood velocity of a few mm/s) and small capillaries randomly distributed in deeper cortical area (diameter lower than 1 μm ; blood velocity below 1 mm/s) [10]. The accurate detection of blood vessels is of prime importance to better understand the functional organization of the brain in normal and pathologic conditions. Indeed, brain activity depends on a continuous supply of oxygen and glucose through cerebral blood flow. Whereas small vessel disease is the most frequent subtype of cerebrovascular cognitive impairment, they are poorly understood due to the lack of medical devices to efficiently image microvasculature. Another benefit of measuring small vessel hemodynamics is to get a dynamic view of the brain in action. Indeed, it has been extensively demonstrated that during of specific task, local neuronal activity has to be matched with a concomitant increase in local cerebral blood flow, a phenomenon called neurovascular coupling that occurs mainly in capillaries [11].

In the recent years, 2 strategies have been developed for ultrasound functional imaging in rodents. The first strategy relies on the use of contrast agents (micro bubbles) combined with high frequency ultrasound (> 20 MHz) to investigate cerebral micro vascular hemodynamics through a cranial window in head fixed [12] or freely moving [13]. The second strategy is based on a ultrasound sequence called functional ultrasound that is sensitive enough to detect blood flow in arterioles and venules without the need for contrast agents [14]. This method was initially limited to craniotomized rodents but has been recently extended to chronic imaging through a thinned skull window [15].

Despite a much greater sensitivity than with conventional Doppler ultrasound, the functional ultrasound method does not measure blood velocities below 4 mm/s that are excluded by the clutter filter [16]. Therefore functional ultrasound can detect neither capillaries nor smallest blood vessels. To overcome this limitation, we present in this letter a spatiotemporal filter based in Single Value Decomposition (SVD) that allows measurement of the slowest blood velocities from functional ultrasound data.

Materials and Methods

Before going into more details about filtering of the data, we will present the experimental set-up and the working principle of functional ultrasound acquisition. In vivo data were collected on adult male Sprague-Dawley rats (Janvier Labs, France) weighing 200–300 g. All animals were used for this study and

were kept in a 12-h dark/light cycle environment at a temperature of 22°C with ad libitum access to food and water. The investigation was performed in accordance with the National Institutes of Health Guide for Care and Use of Laboratory Animals. The protocol was approved Local Animal Ethics Committee of Paris Descartes (CEEA 34) registered with the French Ministry of Research and conducted in accordance with Directive 2010/63/EU of the European Parliament.

Adult rats were anesthetized with 5% isoflurane (Virbac, France) for 5 min in an anesthesia chamber and then reduced to 2.5% isoflurane prior to surgery. The head was fixed in a stereotaxic frame and the scalp was shaved, cleaned with betadine and then removed over the entire dorsal skull. A partial craniotomy was carefully performed to keep the dura intact after removal of the skull bone over the somatosensory cortex (from bregma +0.50 to +3.00 mm and lateral \pm 5.00 mm). The brain surface was protected with 2% ringer-lactate agarose (Lavoisier, France) before brain imaging. The level of the anesthesia was maintained at 1.5% during the rest of the experiment.

All images were acquired using a research ultrasound system. This scanner is composed of an electronic module for ultrasound emission and reception (V1, Verasonics, USA), a linear array transducer with a central frequency of 15 MHz (L15-128, 128 elements, 0.1 mm pitch, Vermon, France) and a computer workstation equipped with 2 GPU (GeForce GTX780Ti, Nvidia, USA) to reconstruct the images in real time.

A functional ultrasound sequence acquires a set of ultrasound images of the brain at a frame rate of 500 Hz. More details about this sequence can be found in [16]. The starting point of our analysis is the set of images $a(x, z, t)$ generated by the μ -Doppler sequence where z is the depth ($n_z = 96$ points spaced 100 μm apart), x is the lateral distance ($n_x = 128$ points spaced 100 μm apart) and t is the time ($n_t = 400$ instants of 2 ms each). These images are composed of 2 parts: echoes from tissue and from blood. $a = a_{Tiss} + a_B$.

The blood flow generates an angular Doppler frequency of

$$\omega_D = 2v \cos\theta \omega_{us} / c \quad (1)$$

Where v is the blood velocity, θ is the angle between the blood velocity and the direction of ultrasound propagation, c is the sound speed and ω_{us} is the angular frequency of the ultrasound wave.

As the tissue is quasi-static, $a_{Tiss}(x, y, z)$ has low frequency components and can be eliminated by using a high-pass filter with cut-off angular frequency ω_{cut} . The cut-off frequency must eliminate all tissue movements due to animal breathing, cardiac pulsation and vibrations of external sources. Previous experiments performed at the same ultrasound frequency required

a 75 Hz cut-off frequency filter. Consequently the μ -Doppler sequence can only quantify the fraction of CBV flowing with an axial velocity higher than 4 mm/s [16]. In these conditions, it was not possible to image neither capillaries nor many small vessels with flow rates below 4 mm/s [9-10].

Because the slow velocities cannot be detected by using the frequency difference between the blood part a_B and the tissue part a_{Tiss} , our solution was to use another physical difference between these two signals. A movement is propagated in the tissue by mechanical waves including compression waves typically travelling at the propagation speed of the medium (approx. 1500 m/s for soft tissue) and shear waves with a speed of a few meters per second. The wavelength of these mechanical waves is very high compared to the size of vessels. For example at 100 Hz, the wavelength is 1 cm for the shear wave and 15 m for the compression wave. As a conclusion, all the tissue at the scale of 1 cm moves coherently. On the contrary, the vascular signal comes from the moving red blood cells that flows randomly inside the vessel and generates a signal that is uncorrelated between two different pixels. This difference can be used to dissociate the tissue from the vessels by computing the signal that is spatially coherent.

An efficient method to identify the coherent part of the signal is to decompose it using a SVD as:

$$a(x, z, t) = \sum_{i=1}^N \lambda_i m_i(x, z) s_i(t) \quad (2)$$

Note that to perform this decomposition the 3D matrix $a(x,y,z)$ must be converted into a 2D matrix $a(k,t)$ where $k=x+zn$ is the spatial part.

The SVD decomposition gives $a(k,t) = \sum_{i=1}^N \lambda_i m_i(k) s_i(t)$ and finally the vector $m_i(k)$ is transformed in a 2D matrix $m_i(x,y)$.

Equation 2 has a simple interpretation: the matrix $m_i(x,y)$ that gives the spatial distribution of the signal $S_i(t)$ for the corresponding singular value. A spatial coherent signal results in a distribution that is widespread in the whole image but an incoherent blood signal is only present in some pixels.

Results and Discussion

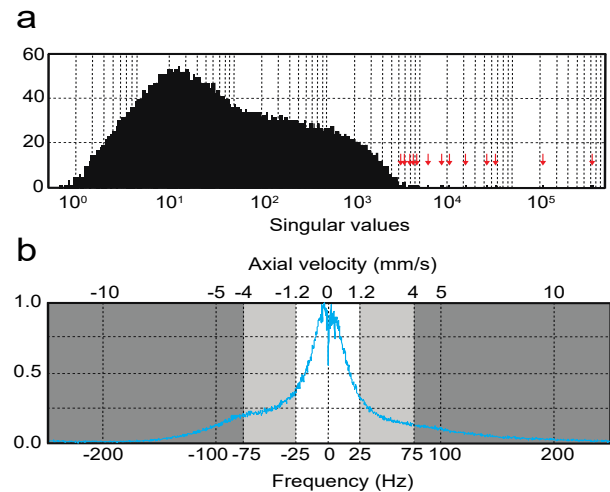
Figure 1a presents a distribution of the singular values for a typical experiment using Doppler ultrasound imaging of a rat brain in resting state. As shown, the distribution is continuous but 12 remarkable high values are located outside the main distribution (arrows). If we remove these values, it is possible to suppress the coherent part of the signal and therefore the blood signal becomes

$$a_B(x, z, t) = \sum_{i=N_e}^N \lambda_i m_i(x, z) s_i(t) \quad (3)$$

Where N_e is the number of eliminated singular values

The spectrum of a_B obtained after the SVD filter is shown in Figure 1b. We divided this spectrum in three bands according to their frequency: below 25 Hz (in white), from 25 to 75 Hz (in light grey) and over 75 Hz (in grey). The low frequency band represents axial velocities below 1.25 mm/s that are mainly observed in capillaries accounting for around 62% of the blood signal intensity. The high frequency band (in grey) defines the detection threshold that was used in previous study [14]. It corresponds to blood vessels with axial velocities higher than 4 mm/s but account for only 13% of the intensity of the entire vascular network. The intermediate frequency band corresponds to a mixed population of small arteries and veins with various sizes that account for 25% of the total signal intensity. These results emphasize the importance of blood velocities measurement without high pass filtering to avoid underestimate in the quantification of the power Doppler spectrum because small vessels and capillaries represent a large proportion of the vasculature of the brain.

Figure 1.



(a) Distribution of singular values after SVD decomposition of a functional ultrasound image acquired on the rat brain. Spatially coherent signals corresponding to the tissue movement generate a reduced number of singular values (red arrows) that are 10 to 100 times higher than the mean value of the distribution. (b) Fourier spectrum of the received blood signal for a cortical region after applying the SVD filter.

The image of the microvasculature is called a functional ultrasound image and is obtained by computing the intensity of the blood signal as

$$I(x, z) = \int |a_B(x, z, t)|^2 dt \quad (4)$$

The intensity of the signal is proportional to the number of red blood cells (RBC) and can be equated to cerebral blood volume [17]. Figure 2a presents a typical functional ultrasound image

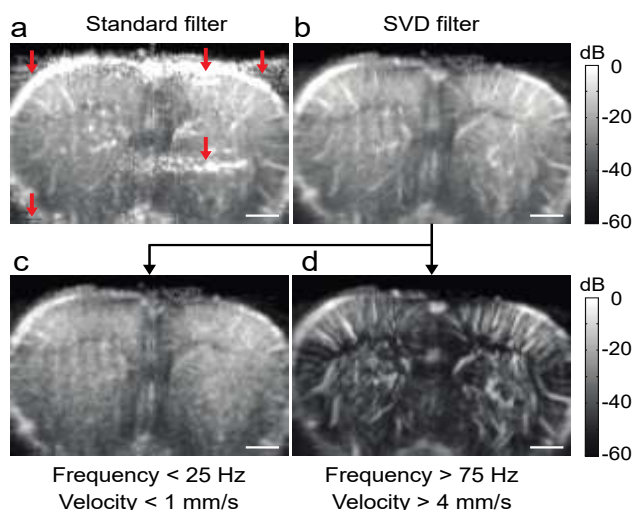
of a rat brain obtained with a standard high-pass filter (Butterworth filter of order 5 with a 25 Hz cut-off frequency). By using this filter, the signal coming from RBC with axial velocity below 1.25 mm/s is lost and the image contains a lot of artifacts due to tissue vibrations (arrows). On the contrary, Figure 2b shows the same dataset computed with a SVD filter offering the full range of RBC velocities without artifacts.

To go deeper into the analysis of Figure 1b, we can split the intensity signal of the functional ultrasound image in 2 distinct bands: a low and a high frequency band using

$$I_{Band}(x, z) = \int_{\omega_{min}}^{\omega_{max}} (A_B(x, z, \omega) + A_B(x, z, -\omega)) d\omega \quad (5)$$

Where A_B is the absolute value of the Fourier transform of a_B , ω_{min} and ω_{max} are the minimal and maximal frequency of the selected band. Note that both positive and negative frequencies are included in Equation 3. Figure 2c and d are derived from Figure 2b and represent a μ -Doppler image of the brain using the low (< 25 Hz) or the high (> 75 Hz) frequency band of the intensity signal, respectively. As a reminder, each voxel has a size of the average size of $100 \times 100 \times 400 \mu\text{m}^3$ and contains a large number of brain capillaries whose size is around 3-4 μm in rodents [18]. In Figure 2c the intensity of the signal is relatively uniform that may indicate a homogeneous mesh size and density of the capillary bed in the entire brain as already observed in monkey [19]. On the contrary, Figure 2d allows the identification of individual large vessels especially in the cortex where they are oriented perpendicularly to the surface of the brain and have a continuous orderly distribution.

Figure 2.

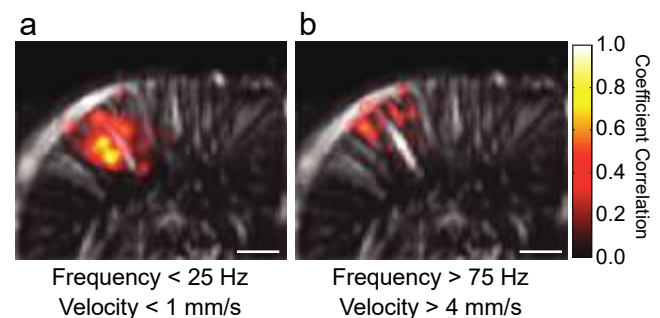


(a) A typical functional ultrasound image of the rat brain obtained with a standard 25 Hz cut-off high-pass filter. A lot of artifacts are presents in the image (red arrows). (b) Same image than in (a) but processed with the SVD filter. The SVD filtered image can be divided in a low frequency band (c) and a high frequency band (d), showing blood in capillaries or larger vessels respectively. Scale bar: 500 μm .

In another set of experiments, we also demonstrated that the use of our SVD filter could also offer significant advantages for the detection of activated regions in functional imaging. Non-noxious electrical pulses (200 μs pulse width, 1 mA intensity, 5 Hz repetition frequency) were delivered using a constant current isolator (DS3, Digitimer Ltd., U.K.) to the right forepaw of anesthetized rats using 2 needle-electrodes (Biopac Systems, Inc., USA) inserted under the palmar skin between digits two and four. Each trial consisted of a 35 s pre-stimulus baseline period followed by a stimulus of 10 pulses (2 s) and a post-stimulus period for a total duration of 50 s. During each trial, the hemodynamic activity of the brain is continuously recorded at a 2 functional ultrasound images per second frequency. Finally, the variation of the signal intensity ΔI is calculated by subtracting the difference between the mean intensity during the 2 s stimulus period minus and the mean intensity during the prestimulus period.

Figure 3a and b are an overlay between the functional ultrasound image and the variation of the signal intensity that is divided according to the low and high frequency bands described previously. Figure 3 shows the large increase of the cerebral blood volume after stimulation of the right forepaw as confirmed by the increase of the Doppler signal intensity in the contralateral somatosensory cortex. Our results also show a spatial segregation of the brain hemodynamic activity according to the frequency band: the slowest velocities (< 1 mm/s) corresponding to the low frequency band are mainly located in deeper cortical structures (layers IV and V), while the fastest velocities band (> 4 mm/s) associated to the high frequency are observed in upper layers I, II and III of the cortex. Moreover, the spatial extent of the activated area is on average around 6 times bigger for capillaries than for penetrating vessels (n=3).

Figure 3.



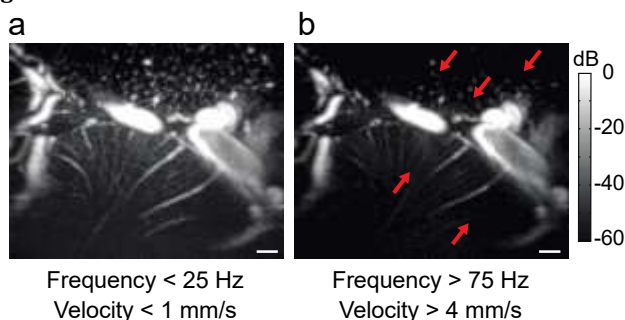
Representative example of functional ultrasound functional activation maps obtained when stimulating the right forepaw in a rat. Only the top left hemisphere of the brain is shown. We calculated maps as the correlation between the stimulus pattern and the power Doppler signal for low (a) or high (b) velocity bands respectively. Scale bar: 500 μm .

We hypothesize that the high velocity band corresponds to the main vessels that primarily drains blood in the activated cortical region while the low velocity band represent the blood volume increase that occurs in capillaries located in the vicinity of the maximal activity of neurons. These results fit those observed with extracellular recording of electrical activity of the brain showing that evoked excitatory postsynaptic potentials are higher in neurons located in layers IV and V of the cortex. Moreover, recording of brain capillaries lead to more accurate images of the brain activity because it has been recently demonstrated that when sensory input increases blood flow, capillaries dilate before arterioles and are estimated to produce 84% of the blood flow increase [11].

Our final goal was to evaluate the quality of the SVD filter for functional ultrasound imaging of brain hemodynamics in human during neurosurgery. For this experiment, tissue vibrations due to internal and external sources become critical. After the neurosurgeon removes of a part the skull bone and the brain is exposed, the tissue movements due to cardiac pulsation and breathing are stronger than in small animals. Moreover, it is not possible to use an anti-vibration table such as for small animal experiments resulting in the transmission of more mechanical noise to the tissue.

All images presented in this study were obtained from patients operated at the Neurosurgery Department of Sainte-Anne Hospital, Paris. Informed and written consent was obtained in all cases following the standard procedure at Sainte-Anne Hospital from patients who were undergoing surgical intervention. Figure 4a and b show images of the human cortical vasculature observed in the middle temporal gyrus and processed in real-time with either a SVD filter or a standard 75 Hz clutter filter, respectively. When comparing both images, we can observe that in the upper part of the image, there is a major reduction of the number of small spots in Figure 4b corresponding to microvessels that are oriented perpendicularly to the imaging plane.

Figure 4.



A functional ultrasound images of the human brain cortical vasculature observed in the middle temporal gyrus and processed in real-time with either a SVD filter (a) or a standard 75 Hz clutter filter

(b). A lot of small vessels disappear when using a 75 Hz high-pass filter (red arrows). Scale bar: 500 μm .

Likewise, we noticed that the number of cortical microvessels that can be observed is significantly reduced by using a 75 Hz high pass filter. Therefore, the SVD filter removes tissue vibrations from functional ultrasound images under difficult experimental conditions (vibrations) but also reveals a large part of brain microvasculature with an unprecedented sensitivity.

Conclusion

To summarize, we use a spatiotemporal SVD filtering algorithm leading to efficient suppression of the clutter signal that is potentially applicable for a wide array of applications in medical imaging. The present work was focused on imaging the blood flow in brain capillaries with functional ultrasound, which were not accessible using conventional clutter filtering methods. We performed for the first time quantitative measurement of brain hemodynamics by measuring than capillaries account for 87% of the total cerebral blood volume. Cerebral micro vascular pathology precedes and accompanies cognitive dysfunction and degeneration of neurons. Therefore, functional ultrasound imaging of capillary blood flow may help to better understand cerebral small vessel pathologies such as stroke, aging or neurodegenerative diseases. For clinical applications, real time functional ultrasound imaging of brain microvasculature may be a new tool for neurosurgeon in locating with a better precision the focus of the epileptic seizure.

Acknowledgments

The authors appreciate help of Emilie Mace in editing the manuscript. The authors thanks Freddy Urban for his help with the 3D design of the ultrasound probe holder. This work was sponsored by a Fondation de l'Avenir grant (ET3-689).

References

1. Yoo YM, Managuli R, Kim Y. Adaptive clutter filtering for ultrasound color flow imaging. *Ultrasound Med Biol*. 2003, 29(9): 1311-1320.
2. Bjaerum S, Torp H, Kristoffersen K. Clutter filter design for ultrasound color flow imaging. *IEEE Trans Ultrason Ferroelectr Freq Control*. 2002, 49(2): 204-216.
3. Cloutier G, Chen D, Durand LG. A new clutter rejection algorithm for Doppler ultrasound. *IEEE Trans Med Imaging*. 2003, 22(4): 530-538.
4. Kadi AP, Loupas T. On the performance of regression and step-initialized IIR clutter filters for color Doppler systems in diagnostic medical ultrasound. *IEEE Trans Ultrason Ferroelectr Freq Control*. 1995, 42(5): 927-937.

5. Yan L, He J, Hong Y. A Study of Ground Clutter Suppression with a Regression Filter. Signal Processing-8th international Conference. 2006, 4.
6. Gallippi CM, Trahey GE. Adaptive clutter filtering via blind source separation for two-dimensional ultrasonic blood velocity measurement. Ultrason Imaging. 2002, 24(4): 193-214.
7. Kruse DE, Ferrara KW. A new high resolution color flow system using an eigendecomposition-based adaptive filter for clutter rejection. IEEE Trans Ultrason Ferroelectr Freq Control. 2002, 49(10): 1384-1399.
8. Mauldin FR, Dan L, Hossack JA. The Singular Value Filter: A General Filter Design Strategy for PCA-Based Signal Separation in Medical Ultrasound Imaging. IEEE Trans Med Imaging. 2011, 30(11): 1951-1964.
9. Shih AY, Friedman B, Drew PJ, Tsai PS, Lyden PD et al. Active dilation of penetrating arterioles restores red blood cell flux to penumbral neocortex after focal stroke. J Cereb Blood Flow Metab. 2009, 29(4): 738-751.
10. Unekawa M, Tomita M, Tomita Y, Toriumi H, Miyaki K et al. RBC velocities in single capillaries of mouse and rat brains are the same, despite 10-fold difference in body size. Brain Res. 2010, 1320 : 69-73.
11. Hall CN, Reynell C, Gesslein B, Hamilton NB, Mishra A et al. Capillary pericytes regulate cerebral blood flow in health and disease. Nature. 2014, 508(7494): 55-60.
12. van Raaij ME, Lindvere L, Dorr A, He J, Sahota B et al. Functional micro-ultrasound imaging of rodent cerebral hemodynamics. NeuroImage. 2011, 58(1): 100-108.
13. Urban A, Dussaux C, Martel G, Brunner C, Mace E et al. Real-time imaging of brain activity in freely moving rats using functional ultrasound. Nat Methods. 2015, 12(9): 873-878.
14. Mace E, Montaldo G, Cohen I, Baulac M, Fink M et al. Functional ultrasound imaging of the brain. Nat Methods. 2011, 8(8): 662-664.
15. Urban A, Mace E, Brunner C, Heidmann M, Rossier J et al. Chronic assessment of cerebral hemodynamics during rat forepaw electrical stimulation using functional ultrasound imaging. NeuroImage. 2014, 101: 138-149.
16. Mace E, Montaldo G, Osmanski BF, Cohen I, Fink M et al. Functional ultrasound imaging of the brain: theory and basic principles. IEEE Trans Ultrason Ferroelectr Freq Control. 2013, 60(3): 492-506.
17. Rubin JM, Bude RO, Fowlkes JB, Spratt RS, Carson PL et al. Normalizing fractional moving blood volume estimates with power Doppler US: defining a stable intravascular point with the cumulative power distribution function. Radiology. 1997, 205(3): 757-765.
18. Blinder P, Tsai PS, Kaufhold JP, Knutsen PM, Suhl H et al. The cortical angiome: an interconnected vascular network with noncolumnar patterns of blood flow. Nat Neuroscience. 2013, 16(7): 889-897.
19. Weber B, Keller AL, Reichold J, Logothetis NK. The microvascular system of the striate and extrastriate visual cortex of the macaque. Cereb Cortex. 2008, 18(10): 2318-2330.